ISSN 1330-3651 (Print), ISSN 1848-6339 (Online)
https://doi.org/10.17559/TV-20250311002458
Original scientific paper

Obtaining of Thermal, Vibration, Air Flow Speed and Performance Analysis of Stator Fin Failure of Three Phase Squirrel Cage Induction Motor

Asım Gökhan YETGİN*, Yusuf Emre ÇAKMAK

Abstract: Under normal operating conditions, induction motors reach a higher temperature value than the initial operating temperature. The higher this temperature value is, the more the losses in the motor increase, negatively affecting the performance of the motor. The increased heat needs to be removed from the motor. There are several ways to do this, the most commonly used of which are the use of fans, fins in the stator frame and fins in the rotor end ring. In this study, the cooling fins in the stator frame of an induction motor were spiraled to create a faulty motor frame. The focus of the study is to experimentally obtain the effects of thermal analysis on the faulty motor body. In addition, performance analyses, vibration analyses and air flow analyses of the motor were performed. These four analyses obtained from the faulty motor were compared with the healthy motor. In order to obtain the data, the motor was tested in no-load, short circuit and loaded operation. The data obtained showed that the temperature values in the faulty motor casing were 6.22% higher in short-circuit operation and 7.95% higher in loaded operation compared to the healthy motor, and accordingly, the performance was adversely affected. The absence of stator fins in the faulty motor caused an asymmetrical distribution of airflow and the difference between inlet and outlet airflow speed decreased by 43%. In addition, it was determined that the faulty motor operated with 1.5-2 times more vibration.

Keywords: air flow speed; induction motor; performance analysis; stator fin failure; thermal analysis, vibration analysis

1 INTRODUCTION

Induction motors are widely used in both commercial and industrial applications [1]. Simplicity, robustness [2] reliability, low manufacturing and maintenance costs [3], high starting torque, adequate speed regulation and reasonable overload capacity [4] are the main reasons for the widespread use of induction motors. In order for an induction motor to operate smoothly under nominal operating conditions, the motor design must first be done properly. After the design phase, critical points such as motor performance, vibration, magnetic calculations, etc. must be controlled. In recent years, in addition to these analyses, thermal analyses of the motor have also begun to be performed. In particular, the stator and rotor winding temperature values have a significant effect on motor efficiency [5]. It should also be noted that the temperature is inversely proportional to the motor lifespan. Cooling is done by various methods in induction motors. These are stator fins placed in various numbers and sizes on the stator frame, rotor fins placed on the rotor end ring and the fans providing natural cooling. These cooling types and motor parts are given in Fig. 1. Several methods adopted for motor cooling include air cooling, liquid cooling and forced convection cooling [6].

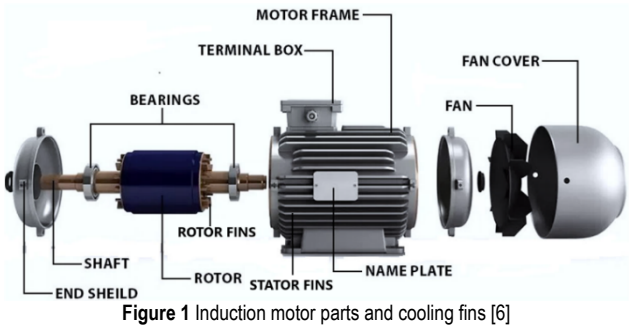

Figure 1 Induction motor parts and cooling fins [6]

In order to guarantee stable operation of squirrel cage induction motors, it is important that the rotor temperature remains at certain levels. Overheating of the rotor seriously affects the end rings and rotor bars. Factors such as severe overload, long-term starting or impaired cooling conditions during operation (due to a broken cooling fan or a clogged motor casing) can affect the cooling capacity of the motor. In this case, the temperature of the rotor bars and end rings, the stator windings and their insulation can exceed the maximum threshold values [7]. Konda et al. have stated that the negative effects of a temperature increase that may occur in induction motors on the motor are as follows: Damage to the stator winding insulation, decrease in motor efficiency, decrease in torque, decrease in motor lifespan, increase in winding impedance, and deterioration of the bearing lubrication system [7]. Albana et al. made a comparison of six different fin designs and studied their effect on the thermal characteristics of the electric motor. The fins were mounted radially and axially. The six types of fin designs investigated were radial fin-round, radial fin-square, radial fin-servo, axial fin-round, axial fin-square and axial fin-servo. The findings of the study showed that the performance of fins in cooling the electric motor depends on the fin area. It was also stated that axially mounted fins provide better cooling than radially mounted fins [8]. Appadurai et al. analyzed the effect of cooling fins on the stator frame of an induction motor using ANSYS program. They examined the temperature changes in the motor frame by changing the number and height of the fins. From the results, they stated that the fin efficiency increased due to the higher length and number of fins, but the volume of the fins also increased, which led to a higher motor mass. From the results, they showed that optimum efficiency and minimum temperature at the fin tip were obtained by using 44 fins with a fin length of 15 mm [9]. Abdullah and Ali investigated the effects of the fins on the stator body of a 2.2 kW induction motor on the motor temperature. They showed that the fin thickness did not have a noticeable difference in motor temperatures, but with the increase in fin depth, there was a significant decrease in temperature values. They also found that the width between the fins had no effect on the motor temperature, and with the increase in the number of fins, there was a significant decrease in the stator winding temperature. They showed that in the absence of any fins

on the stator frame, higher temperature values were obtained in motor temperatures compared to motors with fins [10]. Ulbrich et al. investigated the effect of the number of fins on the motor temperature. It was shown that the temperature decreased with the increase in the number of fins [11]. Wernik stated that the fined motor frame can be applied to prevent emergency situations such as rotor failure that may occur during motor overload. He also stated that the fins will improve cooling efficiency by increasing the heat transfer surface and the heat distribution will be more uniform [12]. Ghahfarokhi and his colleagues found that the air velocity value, which moves from the fan section to the shaft section through the channels in the frame, decreases as it moves away from the fan, and increases with the increase in speed. They showed that the temperature values at different points of the motor decrease as the speed increases [13]. Roffi et al. investigated the effects of different fan types on airflow and efficiency. It was stated that axial fans, when properly designed, will reduce motor operating temperatures [14]. Ramesh et al. is to optimize the cooling rate of different types of fins and different types of materials. Three different materials with high thermal conductivity were selected and their analysis was done. Also, the fins in the stator frame were modelled in different designs [15]. Focus is placed on the design/modelling/analysis/failure of fans, which are another cooling device in induction motors [16-20].

When the literature is examined, it is seen that the studies on the dimensions of the stator frame fins in induction motors have examined their effects on the temperature of the motor. In addition, there are also studies on the effects of the fins on the air flow. It is seen that most studies either examine thermal analyses or only air flow velocities. In this study, in addition to the studies in literature, the main motivation of the study is to obtain a complete analysis by examining the stator fin fault of the three-phase induction motor in 4 categories such as thermal, vibration, air flow velocity and performance. In this context, no-load operation, short circuit operation and loaded operation experiments were performed for healthy and faulty motors. Induction motors are widely used in industry. They are exposed to different failures due to electrical, mechanical and environmental effects. In particular, failures such as fan fractures, fractures in the housing, breakage of the legs are frequently encountered. For this reason, this study was carried out in order to show the importance of the fins in the stator housing on motor performance, cooling, airflow speed and vibration.

2 MATERIALS AND METHODS

The motor used in the experiments is a 3-phase, squirrel cage induction motor, source voltage is 380 V, frequency is 50 Hz, motor power is 1100 W, star connected, nominal current value is 2.7 A, 4 poles, stator slot number is 36, shaft diameter is 25 mm, S1 operation, IP55 protection class and F class insulation. The experimental set is given in Fig. 2.

In the experiments, an autotransformer was used for voltage adjustment, a power analyzer was used for power measurements, and torque measurements were obtained by connecting the test set via the load. In addition, a pen-type vibration device was used for vibration measurements, and a Flir E-5 type thermal camera was used for thermal measurements. To ensure a clear view of both the motor and the load, measurements were taken with a thermal camera at a distance of 1 meter from the test table throughout the experiment. The camera has an image frequency of 9 Hz, a measurement range of −20 to +400 degrees Celsius, IP54 class, a measurement accuracy of ±2%, and a thermal resolution of 160 × 120 pixels. Hand-held anemometer was used to measure air flow velocity. In addition, a tachometer, digital measuring instruments, and a Fucolt brake were used as the load.

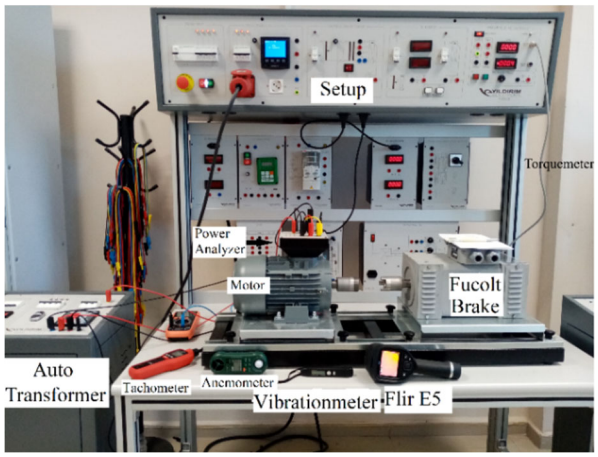

Figure 2 Experimental setup

Fig. 3a shows the image of the healthy motor used in the experiments. Fig. 3b shows the image of the faulty motor with the cooling fins on the stator frame shaved off. The cooling fins were cleaned with a spiral machine. After the fins were spiraled, no cracks etc. occurred on the motor housing, and the roughness on the surface was cleaned with sandpaper afterwards. No damage was caused to the motor housing. The total number of spiraled fins is 17. The fins are parallel to each other and have a length of 98 mm, a width of 15 mm and a depth of 3.25 mm. The distance between the fins is 11.2 mm.

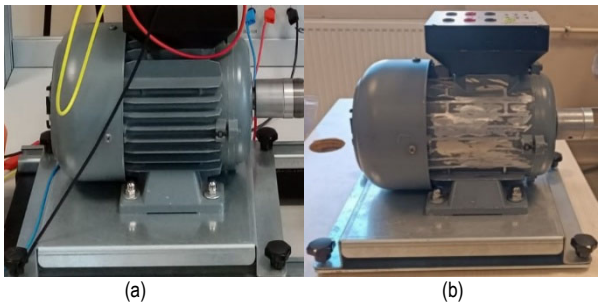

(a) (b)

Figure 3 a) Healthy motor b) faulty motor

3 OBTAINED RESULTS

The results obtained from the thermal, vibration, air flow speed and performance analyses of a healthy and a faulty motor without cooling fins on the stator frame are given below.

3.1 Thermal Tests and Analysis

In the last decade, thermal analysis of electrical machines has received more attention from researchers. In

fact, with the increasing requirements for motor size reduction, energy efficiency, cost reduction and the need to fully utilize new topologies and materials, it is now necessary to analyze the thermal circuit to the same extent as the electromagnetic design [21].

In induction motors, the heat generated in the stator and rotor sections of the motor must be discharged. For this purpose, fins are placed on the stator frame of the motors. In addition, rotor fins placed on end rings and fans are used in the rotor section. In addition, water cooling is also used in specific applications. The cooling fins located in the stator frame help the air coming from the fan to penetrate smoothly from the motor frame to the shaft. A failure in these fins will cause a disruption in the flow of air moving over the frame. This will cause the heat not to be distributed properly and will cause the temperatures on the motor surface and rotor section to increase. This will result in increased losses in the motor and deterioration of motor performance.

The formula giving the resistance change between the initial and final temperature in the motor is given in Eq. (1) [22].

$$R_f = R_i \cdot \left(1 + \alpha \cdot \left(T_f - T_i\right)\right) \tag{1}$$

In the equation, R_i represents the initial resistance value, R_f represents the final resistance value, α represents the temperature coefficient, and T_i and T_f represent the initial and final temperatures, respectively. Here, the temperature coefficient varies depending on the winding material used. Since aluminum is used in the rotor windings, the α value is taken as 0.0038 [23].

The stator winding resistance of the faulty motor at room temperature is 5.2 ohms. When the loaded operation test was completed, the stator winding resistance value was measured as 5.68 ohms. It was determined that the stator winding resistance change between the initial and final temperature values of the motor increased by 9.23%. It was determined that due to the absence of stator cooling fins during the test, an increase occurred in the internal temperature and surface of the motor, and as a result, the stator winding resistance increased. The increase in winding resistance caused an increase in copper losses.

Temperature changes were obtained separately for the healthy and faulty motors during the no-load, short-circuit and loaded tests. The aim here is to show the stator fin effect thermally. Fig. 4a shows the no-load test of the healthy motor, Fig. 4b the short-circuit test, and Fig. 4c the thermal camera images during the loaded test.

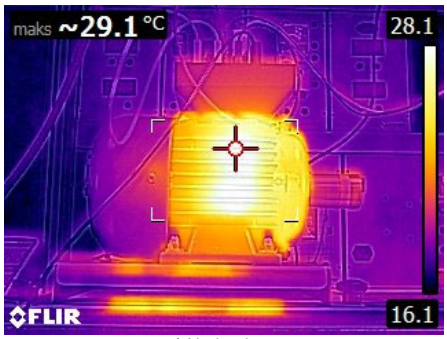

a) No-load test

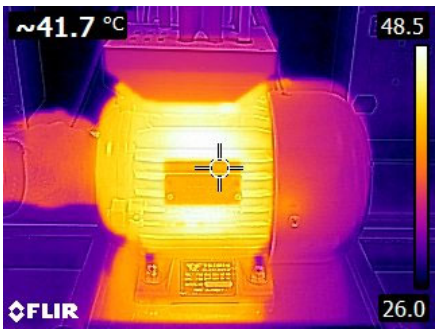

b) Short circuit test

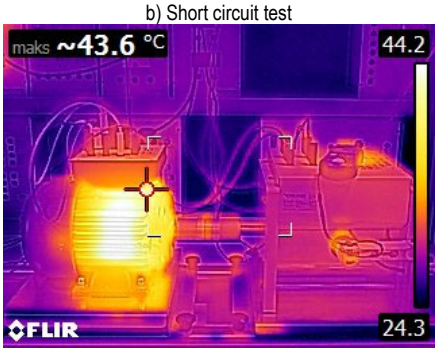

c) Loaded test

Figure 4 Thermal images of the healthy motor

Fig. 5a shows the thermal camera images of the faulty motor during the no-load operation test, Fig. 5b the short circuit operation test, and Fig. 5c the loaded operation test.

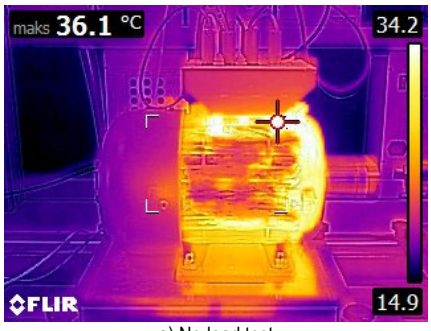

a) No-load test

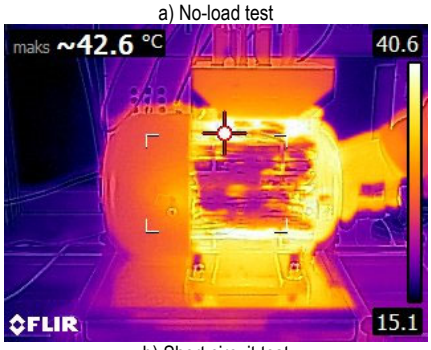

b) Short circuit test

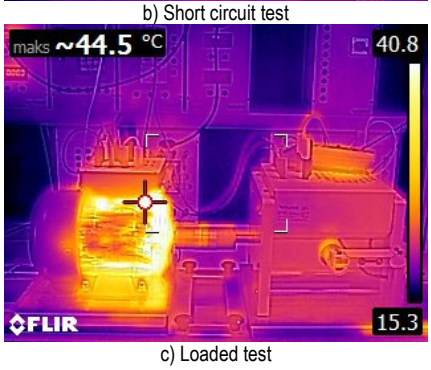

c) Loaded test

Figure 5 Thermal images of the faulty motor

In Fig. 6, the temperature changes of the healthy and faulty motors during no-load and loaded operation are given. An image was taken every 5 minutes, and the experiment duration was set as 25 minutes. The initial temperature was 23 °C, which is the room temperature of the laboratory. When the figure is examined, it is seen that the temperature values increase with the increase in time. In the no-load operation test, since the current value is not very high, the temperature values are seen to be around 33 °C for the healthy motor and 39 °C for the faulty motor. During the loaded operation, it is seen that the temperature values increase rapidly. Especially in the faulty motor, it is seen that the temperature values are higher due to the uneven temperature distribution. In the loaded operation, it was determined that the temperature value of the faulty motor was 7.95% higher than the temperature value of the healthy motor at the 25th minute. This result clearly shows the importance of the fins in the stator frame in cooling the motor.

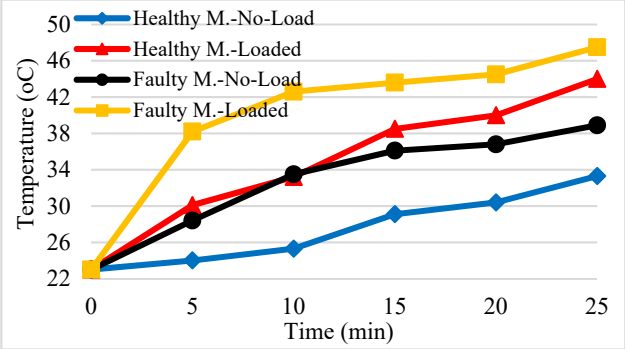

Figure 6 Time-temperature changes of the healthy and faulty motor during no-load and loaded operation

Fig. 7 shows the time temperature changes during short circuit operation for healthy and faulty motors. The test period was set to 70 seconds due to the high current value drawn during short circuit operation. Again, the initial temperature value was 23 °C. When the figure is examined, it is seen that the temperature increases rapidly especially after the 30th second and the temperature values exceed the temperature values in no-load and loaded operation in a very short time. The temperature difference between the faulty motor and the healthy motor at the 70th second is 6.22%.

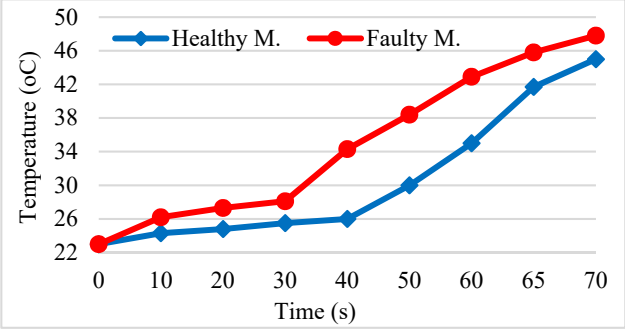

Figure 7 Time-temperature changes in short circuit operation of healthy and faulty motors

The temperature images and graphs obtained show that the failure of the cooling fins located in the stator frame results in an increase in temperatures inside and outside the motor, which negatively affects motor performance.

3.2 Performance Analysis

Another critical point in induction motors is the analysis of the motor's performance values (equivalent circuit parameters, torque values, efficiency, etc.). Performance evaluation was made for both healthy and faulty motors by performing no-load, short-circuit and load operation tests. The tests were carried out under the nominal operating conditions of the motors. The no-load and short circuit operation test results obtained for HealthyMotor (H.M.) and Faulty Motor (F.M.) are given in Tab. 1.

Table 1 Analysis of data obtained from no-load and short circuit tests of healthy and faulty motors

Parameters	No-load test		Short circuit test	
	H.M.	F.M.	H.M.	F.M.
Voltage / V	380	380	85,4	88,7
Current / A	1,72	1,73	2,7	2,7
Power / W	170	174	283	303
Power factor	0,15	0,15	0,71	0,73
Speed (/ rpm	1498	1497	0	0

When Tab. 1 is examined, it is seen that the values obtained in no-load operation are close to each other. A slight increase was observed in iron losses due to the increase in temperature. In short circuit tests, the value of winding resistance increased due to the high current, which caused a 7.06% increase in copper losses. The formulas given in Eq. (2) are used to calculate the single-phase equivalent circuit parameters of the induction motor.

$$Z_{eq} = \frac{V_k}{I_k};\ P_{cu} = 3 \cdot I_k^2 \cdot R_{eq};\ X_{eq} = \sqrt{Z_{eq}^2 - R_{eq}^2};$$
$$R_{fe} = \frac{3 \cdot V_0^2}{P_{fe}};\ X_m = \frac{V_0}{I_0 \cdot \mathrm{Sin}_{\varphi}} \tag{2}$$

In the expression, V_k, I_k and P_{cu} express the voltage, current and copper losses in short circuit operation, respectively. V_0, I_0 and P_{fe} express the voltage, current and iron losses in no-load operation, respectively. The parameters Z_{eq}, R_{eq} and X_{eq} express the equivalent impedance, resistance and reactance. R_{fe} is the iron resistance and X_m is the magnetization reactance. If the stator resistance is unknown, the total equivalent resistance value is divided by 2 to obtain the stator and rotor resistances. The same applies to the stator and rotor reactances. In Eq. (3), the efficiency parameter obtained by using the output power, iron losses and copper losses is given.

$$\eta = \frac{P_{out}}{P_{out} + P_{fe} + P_{cu}} \tag{3}$$

The expression for torque (T) calculated using equivalent circuit parameters in induction motors is given in Eq. (4). In the expression, p indicates the number of poles, s indicates the slip value, R_1 and R_2 indicate the stator

and rotor resistance, and X_1 and X_2 indicate the stator and rotor reactance, V_1 indicate fundamental voltage.

$$T = \frac{3 \cdot p}{2 \cdot \pi * f} \cdot \frac{R_2}{s} \cdot \frac{V_1^2}{\left(\left(R_1 + \frac{R_2}{s} \right)^2 + \left(X_1 + X_2 \right)^2 \right)} \quad (4)$$

Equivalent resistance, reactance and impedance changes of healthy and faulty motors are given in Fig. 8. Units are given in ohms.

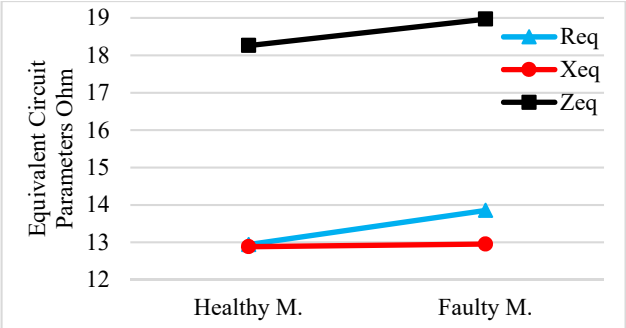

Figure 8 Changes in equivalent circuit parameters of healthy and faulty motors

It is understood that the absence of cooling fins on the stator frame caused the winding resistance of the faulty motor to increase. Because, although the values obtained from the no-load test and the calculations were close to each other in the experiments under the same conditions, the fact that the temperature on the motor could not be properly transferred to the frame and the heat could not be removed from the frame by means of fins caused the values obtained from the short circuit test and the equivalent circuit resistance to be higher.

In addition, it was determined that the iron resistance and magnetization reactance values obtained from the no-load operation experiment were 849.411 ohm and 387.310 ohm for the healthy motor, and 829.885 ohm and 385.071 ohm for the faulty motor, respectively. These results show that the values obtained in the no-load operation are very close to each other and the thermal effect is at a minimum level.

Using the obtained data, the efficiency values of the healthy motor and the faulty motor were calculated as 70.83 and 69.75, respectively. It was determined that the efficiency value decreased by 1.524%. From here, it was determined that since the heat could not be discharged in the faulty motor without fins in the stator frame, thermal losses increased due to the increase in the motor winding resistance values, and the motor performance was negatively affected.

Another performance indicator of the motor, the normalized torque-speed characteristic curve, is given in Fig. 9 for the healthy and faulty motor. When the graph is examined, it is seen that the motor parameters that change with temperature have a significant effect on the torque. It is seen that there are differences especially in the starting and nominal torque values. It is seen that the maximum torque values are close to each other, but similar results are obtained at different speed values. The nominal torque value of the faulty motor was found to be 6.276% lower than that of the healthy motor. In terms of starting torques, the starting torque of the faulty motor was found to be 3.632% higher. When the performance values of the healthy and faulty motor are considered, it is understood that the fins on the motor frame affect the motor performance quite a lot.

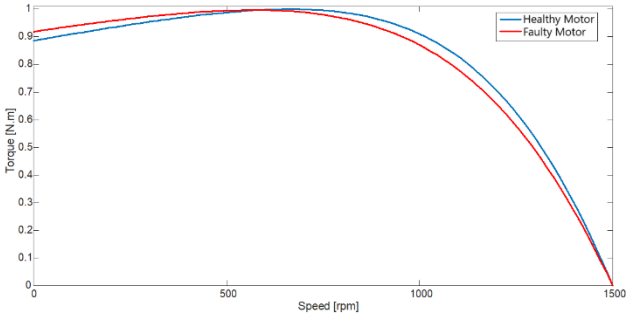

Figure 9 Torque- speed graph of healthy and faulty motor

3.3 Air Flow Velocity Tests and Analysis

In electrical machines, the fins on the stator frame, the fins on the rotor end ring and the fan are used as cooling systems. In addition, water cooling is also used in some special motors. Another subject examined in this study is the analysis of air flow values for healthy and faulty motors. The effect of shaving the fins on the stator frame on the air flow change on the frame was investigated.

The healthy motor cools the motor frame by passing the air drawn in by the fan over the fins. The air flow over the motor is shown in Fig. 10a. The air entering from the fan section takes the heat from the rotor and stator windings and is transferred to the outside through the fins on the frame. Failure to discharge the heat will cause an increase in the temperature value, especially in the stator windings, and this will cause an increase in the winding resistances. In Fig. 10b, it is seen that the air entering from the fan section cannot proceed to the shaft section due to the absence of fins in the stator frame, and the air flow decreases and is distributed in the middle parts of the motor [24].

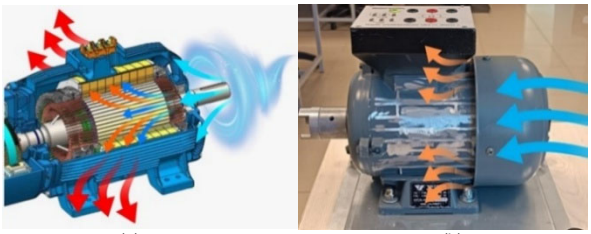

(a) (b)

Figure 10 a) Air flow in a healthy motor b) Air flow in a faulty motor

In Fig. 11a, three points are given where the air flow speed is measured on the motor. Point A is at the rear of the motor and the measurement is taken from the parts where the fins start, point B is at the middle of the motor and the measurement is taken between the fins, and point C is at the end of the fins. In Fig. 11b, three points are given where the motor vibrations are measured. Measurement point 1 is located on the rear cover of the motor, measurement point 2 is located on the front cover of the motor, and measurement point 3 is located on the side of the motor feet, measured from the tabletop. Measurements were made with a pen-type vibration device.

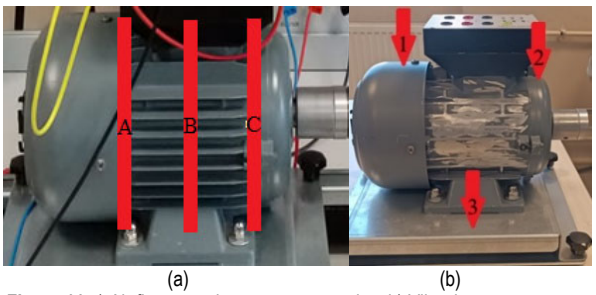

(a) (b)

Figure 11 a) Air flow speed measurement points b) Vibration measurement points

Average air flow speed for healthy and faulty motors is given in Tab. 2 for no-load and loaded operation. While the no-load speed of the motors was around 1497 rpm, the speeds during loaded operation were measured as 1430 rpm and 1427 rpm.

Table 2 Average air flow speed changes of healthy and faulty motors / m/s

Parameters	No-Load Test		Loaded Test	
	Healthy motor	Faulty motor	Healthy motor	Faulty motor
Motor speed / rpm	1498	1497	1430	1427
Air speed at input (Point A)	3,2	3,2	2,7	2,6
Air speed at middle (Point B)	2,9	2,5	2,4	2,0
Air speed at output (Point C)	2,2	1,8	2,0	1,5

When Tab. 2 is examined, it is seen that the air flow speeds measured from the point where the air enters the channels (point A) during the no-load and loaded operation tests are equal. It is seen that the air flow speed values for the faulty motor decrease more around the B value, which is the middle point of the motor. In the measurements made at point C, that is, towards the shaft part of the motor, it is seen that the air flow speed values obtained from both the no-load and loaded operation tests of the faulty motor decrease considerably. These results show that due to the absence of fins in the stator frame, it has been determined that the air moving from the fan to the shaft is quickly dispersed to the sides and cannot penetrate to the shaft parts of the motor. According to the no-load and loaded operation data of the faulty motor, it has been determined that there is a decrease of 43.75% and 42.30% in the air flow speeds entering and exiting the frame part of the motor, respectively. In addition, according to the data obtained, it is seen that since there is a decrease in the speeds of the motors in loaded operation, the air flow values entering the fan part also decrease.

3.4 Vibration Tests and Analysis

The average vibration values obtained from the no-load and loaded operation tests for the healthy and faulty motors are given in Tab. 3.

Table 3 Average vibration values (m/s^2) in no-load and loaded operation tests of healthy and faulty motors

Experiments	Point 1		Point 2		Point 3	
	H.M.	F.M.	H.M.	F.M.	H.M.	F.M.
No-load test	1,9	3,72	2,31	3,96	2,44	4,08
Loaded test	2,1	4,2	2,36	4,3	2,58	4,53

When Tab. 3 is examined, it is seen that the vibration values obtained for both experiments of the healthy motor vary between 1.9-2.58 m/s^2. It is seen that the vibration values obtained in the loaded operation are higher than the values in the no-load operation. It is seen that the vibration values for the no-load operation test of the faulty motor are lower than 4 m/s^2 at locations 1 and 2, while the values are higher in the loaded operation test. The main reason for this situation is that the motor and load shafts are coupled, and an extra vibration comes to the motor from here. When the values at point 3 are compared, it is understood that the vibrations in the motor are transferred to the table by means of the feet. According to the values obtained from 3 different vibration points, the fact that the faulty motor does not have fins caused the motor to operate unbalanced. It is seen that the faulty motor vibration data increases by 1.5-2 times for all three measurement points compared to the healthy motor data.

4 CONCLUSION

In this study, the thermal effects of the cooling fins located in the stator frame of a three-phase squirrel cage induction motor were investigated experimentally. A faulty motor was created by shaving the stator cooling fins. The performance values were obtained by performing no-load, short-circuit and loaded operation experiments of the healthy and faulty motor. At the same time, thermal changes in the motor, vibration measurements and air flow speed measurements were also performed while these experiments were being performed. The results obtained showed that the absence of motor cooling fins negatively affected the air flow in the stator frame. The air entering from the fan side could not progress to the shaft part and was dispersed due to the absence of fins. It was determined that during loaded operation of the faulty motor, the airflow speed at the fan inlet was 2.6 m/s, while the airflow speed at the shaft side dropped to 1.5 m/s. This resulted in an increase in motor temperature due to the lack of complete cooling.

The absence of fins also disrupted the balance of the motor, and it operated with vibration. Especially when the average of all three points was taken during loaded operation, it was determined that the faulty motor operated with approximately 85% more vibration than the healthy motor. In addition to all these, the increase in temperature also negatively affected the performance of the motor.

As a result of thermal analysis, an increase in the winding resistance value occurred with the increase in the temperature value of the faulty motor. This resulted in an increase in the lost power value. It was determined that the efficiency of the faulty motor decreased by 1.524%. When the thermal data of the faulty motor in no-load, short circuit and loaded operation were examined, it was determined that the faulty motor operated at higher temperature values than the healthy motor in all three operations. It is observed that during loaded operation, the temperature value at the last measurement point of the faulty motor is 7.95% higher than the healthy motor, and during short circuit, this value is 6.22%.

If a general evaluation is to be made, 4 different analyses were carried out together in the study in addition to the studies in the literature. It was concluded that the

thermal effect of the faulty motor without stator fins was particularly high and that the motor performance was also negatively affected due to this thermal effect.

5 REFERENCES

[1] Bhambere, M. B. & Chaudhari, S. S. (2022). Numerical analysis of heat transfer from perforated fins of an induction motor housing. *IOP Conf. Series: Materials Science and Engineering*, *1259*, 1-7. https://doi.org/10.1088/1757-899X/1259/1/012011

[2] Markovic, M., Petranovic, Z., & Vujanovic, M. (2024). Numerical simulation of asynchronous e-motor with field-circuit coupling. *Engineering Power*, *19*(1), 12-18.

[3] Spasic, Z. T., Radic, M. M., & Dimitrijevic, D. G. (2016). Temperature rise in induction motor windings as the cause of variation in rotational speed of an axial fan. *Thermal Science*, *20*(5), 1449-1459. https://doi.org/10.2298/TSCI16S5449S

[4] Madhavan, S., Raunak, D. P. B., Gundabattini, E., & Mystkowski, A. (2022). Thermal analysis and heat management strategies for an induction motor, a Review. *Energies*, *15*, 1-15. https://doi.org/10.3390/en15218127

[5] Gebauer, M., Blejchar, T., Brzobohaty, T., & Nevrela, M. (2023). Conjugate heat transfer model for an induction motor and its adequate fem model. *Symmetry*, *15*, 1-40. https://doi.org/10.3390/sym15071294

[6] Pandey, G. K., Sikha, S. S., Thakur, A., Yarlagadda, S. S., Thatikonda, S. S., Suja, B. B., Mystkowski, A., Dragasius, E., & Gundabattini, E. (2023). Thermal mapping and heat transfer analysis of an induction motor of an electric vehicle using nanofluids as a cooling medium. *Sustainability*, *15*, 1-18. https://doi.org/10.3390/su15108124

[7] Konda, Y. R., Ponnaganti, V. K., Reddy, P. V. S., Singh, R. R., Mercorelli, P., Gundabattini, E., & Solomon, D. G. (2024). Thermal analysis and cooling strategies of high-efficiency three-phase squirrel-cage induction motors-a review. *Computation*, *12*(6), 1-21. https://doi.org/10.3390/computation12010006

[8] Albana, M. H., Guntur, H. L., & Putra, A. B. K. (2023). The effect of fins design on the thermal characteristics of electric motors for electric vehicles. *International Conference on Advanced Mechatronics, Intelligent Manufacture and Industrial Automation (ICAMIMIA)*, 1-6. https://doi.org/10.1109/ICAMIMIA60881.2023.10427619

[9] Appadurai, M., Raj, E. F. I., & Venkadeshwaran, K. (2021). Finite element design and thermal analysis of an induction motor used for a hydraulic pumping system. *Materials Today: Proceedings*, *45*, 7100-7106. https://doi.org/10.1016/j.matpr.2021.01.944

[10] Abdullah, A. T. & Ali, A. M. (2019). Thermal analysis of a three-phase induction motor with frame design considerations. *IOP Conf. Series: Materials Science and Engineering*, *518*, 1-10. https://doi.org/10.1088/1757-899X/518/4/042010

[11] Ulbrich, S., Kopte, J., & Proske, J. (2018).Cooling fin optimization on a tefc electrical machine housing using a 2-D conjugate heat transfer model. *IEEE Transactions on Industrial Electronics*, *65*(2), 1711-1718. https://doi.org/10.1109/TIE.2017.2748051

[12] Wernik, J. (2017). Investigation of heat loss from the finned housing of the electric motor of a vacuum pump. *Applied Science*, *7*(12), 1-9. https://doi.org/10.3390/app7121214

[13] Ghahfarokhi, P. S., Kallaste, A., Podgornovs, A., Belahcen, A., Vaimann, T., & Asad, B. (2021). Determination of heat transfer coefficient of finned housing of a tefc variable speed motor. *Electrical Engineering*, *103*, 1009-1017. https://doi.org/10.1007/s00202-020-01132-1

[14] Roffi, M., Ferreiraet, F. J. T. E., & De Almeida, A. T. (2017). Comparison of different cooling fan designs for electric motors. *IEEE International Electric Machines and Drives Conference*, 1-7. https://doi.org/10.1109/IEMDC.2017.8002270

[15] Ramesh, C., Subbiah, A., Sivakumar, K., & Sri, G. T. (2021). Design and material optimization of cooling fins in electric motors. *Annals of the Romanian Society for Cell Biology*, *25*(5), 1991-2004.

[16] Gallonia, E., Parisia, P., Marignettib, F., & Volpec, G. (2018). CFD Analyses of a radial fan for electric motor cooling. *Thermal Science and Engineering Progress*, *8*, 470-476. https://doi.org/10.1016/j.tsep.2018.10.003

[17] Singh, G., Kumar, T. C. A., & Naikan, V. N. A.(2016). Fault diagnosis of induction motor cooling system using infrared thermography. *IEEE 6th International Conference on Power Systems*, 1-4. https://doi.org/10.1109/ICPES.2016.7584040

[18] Goh, S., Fawzal, A. S., Gyftakis, K. N., & Cardoso, A.J. M. (2018). Impact of the fan design and rotational direction on the thermal characteristics of induction motors. *IEEE XIII International Conference on Electrical Machines*, 1227-1233. https://doi.org/10.1109/ICELMACH.2018.8506974

[19] Kim, C., Lee, K. S., & Yook, S. J. (2016). Effect of air-gap fans on cooling of windings in a large-capacity, high-speed induction motor. *Applied Thermal Engineering*, *100*, 658-667. https://doi.org/10.1016/j.applthermaleng.2016.02.077

[20] Koa, M. J., Leea, S. H., & Park, S. S. (2021). IE4-class 2.2-kW induction motor design and performance evaluation. *Journal of the Korean Society of Manufacturing Technology Engineers*, *30*(5), 345-351. https://doi.org/10.7735/ksmte.2021.30.5.345

[21] Staton, D. A. & Cavagnino, A. (2008). Convection heat transfer and flow calculations suitable for electric machines thermal models. *IEEE Transactions on Industrial Electronics*, *55*(10), 3509-3516. https://doi.org/10.1109/TIE.2008.922604

[22] Marangoni, T. A., Guralnik, B., Borup, K. A., Hansen, O., & Petersen, D. H. (2021). Determination of the temperature coefficient of resistance from micro four-point probe measurements. *Journal of Applied Physics*, *129*, 1-9. https://doi.org/10.1063/5.0046591

[23] Bird, J. (2003). *Electrical Circuit Theory and Technology*. Chapter 3: Resistance Variation, Second Edition, Elsevier Science, Great Britain.

[24] Cakmak, Y. E. (2023). *Experimental investigation of the effects of stator fin fault on the performance of three-phase squirrel cage induction motor*. M.Sc. Thesis, Burdur Mehmet Akif Ersoy University, Burdur, Türkiye.

Contact information:

Asım Gökhan YETGİN
(Corresponding author)
Electrical and Electronics Engineering Department,
Burdur Mehmet Akif Ersoy University, Türkiye
E-mail: agyetgin@mehmetakif.edu.tr

Yusuf Emre ÇAKMAK
Energy Systems Engineering Department,
Burdur Mehmet Akif Ersoy University, Türkiye
E-mail:yusufemrecakmak@gmail.com